YMTHE, Volume *28*

Supplemental Information

miR24-2 Promotes Malignant Progression of Human Liver Cancer Stem Cells by Enhancing Tyrosine Kinase Src Epigenetically

Liyan Wang, Xiaonan Li, Wei Zhang, Yuxin Yang, Qiuyu Meng, Chen Wang, Xiaoru Xin, Xiaoxue Jiang, Shuting Song, Yanan Lu, Hu Pu, Xin Gui, Tianming Li, Jie Xu, Jiao Li, Song Jia, and Dongdong Lu

Supplemental Materials and Methods

Expression plasmid for human miR24-2

Human miR24-2 expression plasmidwas purchased from Origene (CAT#: SC400297). pCMV-miR vector for miRNA expression clone with GFP as reporter expresses microRNA precursors from CMV promoter. The miR24-2 precursor insert was cloned between SgfI and MluI site and Neomycin selection marker for stable cell establishment.

rLV-U6 -miR24-2 sgRNA-Cas9-ZsGreen Lentiviral

Both the vector plasmid pLVX-U6-Cas9-ZsGreen (Wuhan Venuosai Biotechnology Co., Ltd.) and the target gene plasmid pUC57-hsa-miR24-2 sgRNA (CTCTGCCT***CCCGTGCCTACTGAGCTGAA***ACACAGTTGGTTTGTGTACACTG GCTCAGTTCAGCAGGAACAGGG) were double-digested, and the large fragment of plasmid pLVX-U6-Cas9-ZsGreen and the small fragment of plasmid pUC57-has-miR24-2 sgRNA were recovered by 1% agarose gel electrophoresis. The two plasmid fragment was then carried out ligation reaction at 16 ° C for 4 hours, and the ligation product was transformed into JM109 competent bacterial and cultured

overnight. Monoclonal colonies were picked for sequencing verification. The recombinant plasmid pLVX-U6-miR24-2 sgRNA-Cas9-ZsGreen was transfected into 293 T cells to generate a high titer lentivirus containing the gene of interest (rLV-Cas9-miR24-2).

Tetracycline (DOX) inducting lentiviral rLV-tet on-miR24-2

The expression plasmid pLVX-tet on-Tight-EF1a-ZsGreen and the target gene plasmid pUC57-has-miR24-2 were digested with BamHI and NotI, respectively, and the large fragment of plasmid pLVX-tet on-Tight-EF1a -ZsGreen and the small fragment pUC57-miR24-2 were recovered by 1% agarose gel electrophoresis respectively. The two plasmid pLVX-tet on-Tight-EF1a-ZsGreen (BamHI+NotI) and pUC57-miR24-2 (BamHI+NotI) were carried out the ligation reaction at 22 ° C for 3 hours and then the ligation products were transformed t into JM109 competent bacterial overnight. Monoclonal colonies were picked for sequencing verification. The recombinant plasmid pLVX-tet on-miR24-2-Tight-EF1a-ZsGreen containing the

gene of interest was transfected into 293 T cells to generate a high titer lentivirus containing the gene of interest (rLV-tet on miR24-2).

Expression Lentivirus for human miR675

The vector plasmid pLVX-ZsGreen-miRNA-Puro (Wuhan Venuosai Biotechnology Co., Ltd.) and the target gene plasmid pUC57-has-miR675 (MI0005416) were double-digested with BamHI and NotI, respectively, and he large fragment of plasmid pLVX-ZsGreen-miRNA-Puro and the small fragment of plasmid pUC57-has-miR675 was recovered by 1% agarose gel electrophoresis. The two plasmid fragments were performed ligation reaction t at 22 ° C for 3 hours, and the ligation product was transformed into JM109 competent bacterial and cultured overnight. The monoclonal colonies were picked for sequencing verification, and the sequencing primer: ZsGreen-F (5'-GCGACGCCAAGAACCAGAAG-3'). The recombinant plasmid pLVX-ZsGreen-miR675-Puro containing the gene of interest was transfected into 293 T cells, respectively, generating a lentivirus containing a gene of interest at a high titer (rLV-miR675).

rLV-U6 –miR675 sgRNA-Cas9-ZsGreen Lentiviral

Both the vector plasmid pLVX-U6-Cas9-ZsGreen (Wuhan Venuosai Biotechnology Co., Ltd.) and the target gene plasmid pUC57-hsa-miR675 sgRNA (CTGTTAATGCTAATCGTGATAGGGGTTTTTGCCT*CACTGTGGGCCCTCTCC GCACCA*AGCATTAACAG) were double-digested, and the large fragment of plasmid pLVX-U6-Cas9-ZsGreen and the small fragment of plasmid pUC57-has-miR675 sgRNA were recovered by 1% agarose gel electrophoresis. The two plasmid fragment was then carried out ligation reaction at 16 ° C for 4 hours, and the ligation product was transformed into JM109 competent bacterial and cultured overnight. Monoclonal colonies were picked for sequencing verification. The recombinant plasmid pLVX-U6-miR675 sgRNA-Cas9-ZsGreen was transfected into 293 T cells to generate a high titer lentivirus containing the gene of interest (rLV-Cas9-miR675).

Northern-Western blotting for miRNA RNA samples were separated on 15% polyacrylamide/8M urea gel. Soak Hybond-N+ membrane (Amersham Pharmacia,

Uppsala, Sweden) in ddH2O for a few seconds and in transfer buffer (0.5X TBE) for 20 minutes ,and soak two pieces of whatman paper in 0.5XTBE . Separated RNA in gel was electro-blotted onto Hybond-N+ membrane (Amersham Pharmacia, Uppsala, Sweden). After UV cross-linking and air drying, blotted membrane was prehybridized with hybridization buffer at 42 ºC for 60 min, and then hybridized with Biotin-labeled antisense miR24-2 probe and incubated at 42 ºC for overnight. The membrane was washed 4 times at 42 ºC with 2x SSC and 0.5% SDS and then western blotting with anti-Biotin according to the our pervious protocol.

Supplemental Results

The isolation of human liver cancer cell (hLCSCs)

hLCSCs were isolated from human liver cancer cell line Huh7 using CD133/CD44/CD24/EpCAM microbeads(**Fig.S1A**). CD133, CD44, CD24 or EpCAM were positively expressed in hLCSCs and not expressed in non-hLCSCs (**Fig. S1B-D**).

The knockout of miR-24-2 did not affect the expression of miR-23a and miR-27a in liver cancer stem cells

We performed the Northern-Wstern blotting in rLV-Cas9 group and rLV-Cas9 –miR 24-2group and the results showed the there are no significant difference of miR-23a(250bp pri-miR-23a,73bp premiR23a, 22bp mature miR23a) between rLV-Cas9 group and rLV-Cas9 –miR24-2group(**FigureS4A**) and there are no significant difference of miR-27a(262 bp pri-miR-27a,78bp pre-miR27a, 22bp mature miR27a) between rLV-Cas9 group and rLV-Cas9–miR 24-2group (**FigureS4B**).These observations suggest that the knockout of t miR-24-2 did not affect the expression of miR-23a and miR-27a.

miR24-2 accelerates the growth of liver cancer stem cells *in vitro and in vivo.*

The positive rate of BrdU was significantly increased in the pCMV-miR24-2 group compared with the pCMV-miR group (19.46±2.27% vs 63.49±5.57%, P=0.00196) and reduced in the rLV-Cas9-miR24-2 group compared with the rLV-Cas9 group (23.12 ± 3.25% vs 7.01 ± 1.02%, P = 0.00777) (**Fig. S2D**).

Although there was no significant difference in the average scratch width at 0 hours of scratching among the pCMV-miR group, pCMV-miR24-2 group, rLV-Cas9 group, and rLV-Cas9-miR24-2 group (P>0.05), the average width ratio of scratches (24 hours/0 hours) after 24 hours of scratching was significantly reduced in the pCMV-miR24-2 group compared with the pCMV-miR group (0.0975±0.018 vs 0, P=0.0056) and increased the rLV-Cas9-miR24-2 group compared to the rLV-Cas9 group (0.0835 ± 0.0097 vs 0.2437 ± 0.0243, P = 0.00697 < 0.01) (**Fig. S2Ea&b**)

hLCSCs were infected with rLV-tet on-miR24-2, and the positive cells were picked up by several times under a fluorescence microscope, and were expanded. In stable hLCSCs cell lines , including DOX (0 μg/ml) group, DOX (0.5 μg/ml) group, DOX (1 μg/ml) group, DOX (2 μg/ml) group, precursor of miR24-2(pre-miR24-2) and the mature miR24-2 were significantly increased with increase of DOX concentration, and the pri-miR24-2 did not significantly change (**Fig. S2Ha-c**). The cell growth ability was significantly increased with the increase of DOX concentration (P<0.01) (**Fig.S2I**). The colony formation rate was significantly increased with the increase of DOX concentration (37.3±3.81% vs 56.63±5.42%, P=0.02109<0.05; 56.63 ±5.42% vs

70.15±3.02%, P=0.008446<0.01; 70.15±3.02% vs 87.21±7.41%, P=0.01327<0.05) (**Fig.S2J**). The sphere formation rate was significantly increased with the increase of DOX concentration, (15.08±3.45% vs 36.64±4.69%, P=0.00080848<0.01; 36.64±4.69% vs 55.30±5.33%, P=0.00074095<0.01; 55.30±5.33% vs 69.34±6.78%, P=0.0423375< 0.05) (**Fig.S2K**). The average weight of transplanted tumors in nude mice was significantly increased with the increase of DOX concentration (0.32±0.069 g vs 0.6±0.104 g, P=0.004451<0.01; 0.6±0.104).克 vs 0.82 ± 0.081 g, P = 0.0092314 < 0.01; 0.82 ± 0.081 g vs 1.31 ± 0.25 g, P = 0.0020429 < 0.01) **(Fig. S2La-b**). The average appearance time of transplanted tumor in nude mice was significantly decreased with the increase of DOX concentration (9.83±0.98 days vs 7.33±1.21 days, P=0.003374<0.01; 7.33 ± 1.21 days vs 5.67 ± 0.52 days, P = 0.00993 < 0.01; 5.67 ± 0.52 days vs 5.17 ± 0.75 days, P = 0.037779 < 0.05) (**Fig.S2Lc**). Collectively, these observations suggest that miR24-2 accelerates the growth of liver cancer stem cells *in vitro and in vivo.*

miR24-2 targets PRMT7 3 '-UTR and inhibits the expression of the PRMT7 in human liver cancer stem cells

In stable rLV-tet on-miR24-2 infected hLCSCs, including DOX (0 μg/ml) group, DOX (0.5 μg/ml) group, DOX (1μg/ml) group, DOX (2 μg/ml) group, pre-miR24-2 and the mature miR24-2 were significantly increased with increasing DOX concentration, and the pri-miR24-2 did not change significantly (**Fig. S5Ca-c**).Moreover, the binding ability of the mature miR24-2 or AgoII to PRMT7 3'-UTR was significantly increased with increasing DOX concentration (**Fig. S5D**) and the pEZX-MT-PRMT7 3'-UTR-Luc luciferase reporter gene activity were significantly decreased with increasing DOX concentration ($P<0.01$) (**Fig.S5E**). In addition, the pEZX-MT-PRMT7 3'-UTR (mutant)-Luc luciferase reporter gene activity did significantly not change with increasing DOX concentration **(Fig.S5F)**. Although there was no significant change in transcriptional level of PRMT7, the translational level of PRMT7 was significantly reduced as the increasing DOX concentration **(Fig.S5G)**. Taken together, these results suggest that miR24-2 targets PRMT7 3 '-UTR and inhibits the expression of the PRMT7 in human liver cancer stem cells.

miR24-2 affects the modification of trimethylation of arginine-3 of histone H4 on the HULC promoter region specifically

We performed the native CHIP with anti-H4R3me2 and anti-H4R3me3 to confirm the specific modification of dimethylation and trimethylation of arginine-3 of histone H4 on the HULC promoter region. We designed the CHIP primers according to the HULC promoter sequence[AL133261.8 (1..66219)](**FigureS6A**).

As shown in **FigureS6B**a, the modification of dimethylation of arginine-3 of histone H4 on the HULC promoter region of P7-P8 and P9-P10 was significantly decreased in rLV-miR24-2 group compared to rLV group and significantly increased in rLV-Cas9-miR24-2 group compared to rLV-Cas9 group. And the modification of dimethylation of arginine-3 of histone H4 on the HULC promoter region of P5-P6 and P11-P12 was not significantly altered in rLV group , rLV-miR24-2group ,rLV-Cas9 group and rLV-Cas9-miR24-2 group. And there was no the modification of dimethylation of arginine-3 of histone H4 on the HULC promoter region of P1-P2,P3-P4, P13-P14,P15-P16,P17-P18. Moreover, the real-time native CHIP obtained the similar findings(**FogureS6Bb**). Thus, miR24-2 affects the modification

of dimethylation of arginine-3 of histone H4 on the HULC promoter region of P7-P8 and P9-P10 specifically.

As shown in **FigureS6C**a, the modification of trimethylation of arginine-3 of histone H4 on the HULC promoter region of P7-P8 and P9-P10 was significantly decreased in rLV-miR24-2 group compared to rLV group and significantly increased in rLV-Cas9-miR24-2 group compared to rLV-Cas9 group. And the modification of trimethylation of arginine-3 of histone H4 on the HULC promoter region of P5-P6 , P11-P12 and P15-P16 was not significantly altered in rLV group , rLV-miR24-2group ,rLV-Cas9 group and rLV-Cas9-miR24-2 group. And there was no the modification of dimethylation of arginine-3 of histone H4 on the HULC promoter region of P1-P2,P3-P4, P13-P14,P17-P18. Moreover, the real-time native CHIP obtained the similar findings(**FogureS6Cb**). Thus, miR24-2 affects the modification of trimethylation of arginine-3 of histone H4 on the HULC promoter region of P7-P8 and P9-P10 specifically.

miR24-2 promotes the expression and maturation of miR675 via Nanog

In hLCSCs infected with rLV-tet on-miR24-2, both pre-miR24-2 and mature miR24-2 were increased significantly with increasing DOX concentration (**Fig.S7Aa&b**). In particular, the binding ability of Nanog, H3K9Ac and RNA polII to Pri-miR675 promoter cis-elements was significantly increased and the binding ability of HDAC4 to Pri-miR675 promoter cis-elements was significantly decreased with increasing DOX concentration,respectively(**Fig.S7B**).Moreover, the binding ability did significantly not change among rLV-tet on-miR24-2/DOX (0μg/ml) group, rLV-tet on-miR24-2/DOX(2μg/ml)+pGFP-V-RS-Nanog group (**Fig. S7C)**. And the binding capacity of RNApolII to pri-miR675 promoter cis-element probe was increased significantly as the increasing DOX concentration **(Fig. S7Da&b)**,and the binding capacity of RNApolII to the pri-miR675 promoter cis-element probe did significantly not change with increasing DOX concentration among rLV-tet on-miR24-2 /DOX (0μg/ml) group , rLV-tet on-miR24-2 /DOX (1 μg/ml) +pGFP-V-RS-Nanog group, rLV-tet on-miR24-2/DOX (2 μg/ml)+pGFP-V-RS-Nanog group **(Fig. S7Ea&b**). The pEZX-MT-Pri-miR675-Luc luciferase reporter gene activity was increased with increasing DOX concentration

(P<0.05 or P<0.01) (**Fig.S7F**). However, the luciferase reporter gene activity was significantly not changed with increasing DOX concentration among rLV-tet on-miR24-2 /DOX (0μg/ml) group, rLV-tet on-miR24-2/DOX(1μg/ml)+pGFP-V-RS-Nanog group, rLV-tet on-miR24-2/DOX (2μg/ml)+pGFP-V-RS-Nanog group (P>0.05)(**Fig.S7G**).

miR675 targets HDAC3 3'UTR and and inhibits translation of the *HDAC3* gene in human liver cancer stem cells

In hLCSCs infected with rLV, rLV-miR675, rLV-Cas9, and rLV-Cas9-miR675 respectively, the pre-miR675 and mature miR675 were increased in the rLV-miR675 group compared with the rLV group and knocked out in the rLV-Cas9-miR675 group compared with the rLV-Cas9 group (**FigureS8A&B**). Bioinformatics analysis revealed that the mature sequence of miR675 binds to the 3'-noncoding region (UTR) of histone deacetylase 3(HDAC3) mRNA through a 9-base seed sequence (**Fig. S8C**). pEZX-MT-HDAC3 3'-UTR-Luc reporter gene activity was significantly reduced in the rLV-miR675 group compared with the rLV group (P=0.003548<0.01) and significantly increased in the rLV-Cas9-miR675 group compared to rLV-Cas9 (P =

0.0005911< 0.01) (**Fig. S8D**). Although there was no significant change in the transcriptional level of HDAC3 in the rLV-miR675 group or rLV-Cas9-miR675 groups compared to the control group (**Fig. S8E**), the expression of HDAC3 was significantly reduced in the rLV-miR675 group compared to the rLV group and increased in the rLV-Cas9-miR675 group compared to the rLV-Cas9 group (**Fig. S8F)**. These results suggest that miR675 targets HDAC3 3'UTR and and inhibits translation of the *HDAC3* gene in human liver cancer stem cells

PI3K knockdown abrogates these actions of miR24-2 for autophagy

The expression of PI3K, LC3I and LC3II was significantly increased in the pCMV-miR24-2 group compared to the pCMV-miR group. However, there was no significant change between the pCMV-miR24-2+pGFP-V-RS-PI3K group and the pCMV-miR group(**Fig.S11A)**. The expression of PI3K, LC3I and LC3II were significantly increased in the DOX (2 μg/ml) group compared with the DOX (0 μg/ml) group. However, the expression of PI3K, LC3I and LC3II was significantly not changed in the rLV-tet on-miR24-2+pGFP-V-RS-PI3K/DOX (2μg/ml) group compared with the DOX (0 μg/ml) group (**Figure S11B**). The expression of LC3I and

LC3II was significantly increased in the DOX (2 μg/ml) group compared to the DOX (0 μg/ml) group. However, there was no significant change in rLV-tet on-miR24-2 + pGFP-V-RS-KAT8/DOX(2μg/ml) or rLV-tet on-miR24-2+pcDNA3-SET8 compared to the DOX (0 μg/ml) group (**Fig.S11C**). However, the interaction between the LC3 and ATG3 was not significantly changed in the pCMV-miR24-2+pGFP-V-RS-PI3K group compared to pCMV-miR group (**Fig. S11D**). The interaction between the LC3 and ATG3 was significantly increased in rLV-tet on-miR24-2/DOX (2μg/ml) group compared to the rLV-tet on-miR24-2/DOX (0 μg/ml) group. However, there was no significant change between rLV-tet on-miR24-2+pGFP-V-RS-PI3K/DOX (2μg/ml) group and the rLV-tet on-miR24-2/DOX (0 μg/ml) **(Fig.S11E)**. Moreover, the expression of the Beclin1 was significantly increased in the pCMV-miR24-2 group compared with the pCMV-miR group. However, the expression of the Beclin1 was not significantly changed between the pCMV-miR24-2+pGFP-V-RS-PI3K group and pCMV-miR group **(Fig.S11F).** The expression of Beclin1 was significantly increased in rLV-tet on-miR24-2/DOX (2μg/ml) group compared to the rLV-tet on-miR24-2/DOX (0 μg/ml) group . However, there was no significant change

between the rLV-tet on-miR24-2+pGFP-V-RS-PI3K/DOX (2 μg/ml) group and the rLV-tet on-miR24-2/DOX group(**Figure S11G**). The incidence of autophagy was significantly increased in the pCMV-miR24-2 group compared with the pCMV-miR group (10.39±1.76% vs 45.01±6.96%, P=0.008375<0.01). However, the incidence of autophagy was not significantly changed in the pCMV-miR24-2+pGFP-V-RS-PI3K group compared to pCMV-miR group (10.39±1.76% vs 5.93±2.29%, P=0.09818>0.05) **(Fig.S11Ha&b)**. The incidence of autophagy was significantly increased in rLV-tet on-miR24-2/DOX (2μg/ml) group compared to the rLV-tet on-miR24-2/DOX (0 μg/ml) group (5.58±3.01% vs 41.29±7.02%, P=0.00987011<0.01). However, there was no significant change between the rLV-tet on-miR24-2+pGFP-V-RS-PI3K/DOX (2 μg/ml) group and rLV-tet on-miR24-2/DOX(0 μg/ml) group (5.58±3.01% vs 6.85±1.67%, P=0.13632>0.05) **(Fig.S11Ia&b).** Collectively, these results suggest that miR24-2 promotes autophagy dependent on PI3K in human liver cancer stem cells.

Supplemental Figure legends

Figure S1 The isolation and identification of human liver cancer stem cell. **A.** the schematic diagram for isolating liver cancer stem cells from Huh7 liver cancer cell line using CD133/CD44/CD24/EpCAM microbeads (MicroBeads). B. The transcriptional ability of CD133, CD44, CD24, and Epcam was analyzed by reverse transcription polymerase chain reaction, and β-actin was used as an internal reference gene. C. Western blotting analysis using anti-CD133, anti-CD44, anti-CD24, anti-EpCAM, and β-actin as an internal reference gene. D. Comparison of human liver cancer stem cells (hLCSCs) and non-liver cancer stem cells (non-hLCSCs) isolated from human hepatoma cell Huh7 (bar ± SEM, n = 3), * *, $P < 0.01$, *, $P < 0.05$.

Figure S2 miR24-2 promotes growth of human liver cancer stem cells. A. The pCMV-miR or pCMV-miR24-2 were transfected into and the rLV-Cas9 or rLV-Cas9-miR24-2 were infected hLCSCs, respectively, and the positive cells were picked under fluorescent microscope and were expanded. The images taken with a fluorescence microscope (100×) was showed. B. The miR24-2 was detected by DOT-Blotting. U6 was used as an internal reference. C. Back-to-back RT-PCR was

used to detect the circular miR24-2. D. Determination of the S phase of hLCSCs cells by BrdU staining. a. BrdU stained photograph; b. Percentage of S phase cells. E. The wound test . a. Scratch photographs taken at 0 and 24 hours, respectively. b. Comparison of the average width of the scratches of the cells. F.4% formalin-fixed, paraffin-embedded nude mouse transplanted tumor tissue sections (4 μm) were subjected to hematoxylin-eosin (HE) (original magnification × 100). G. 4% formalin-fixed, paraffin-embedded nude mouse transplanted tumor tissue sections (4 μm) were subjected to the immunohistochemical staining of anti-PCNA (original magnification × 100). **H**. a. Northern-western blotting was used to detect the miR24-2.U6 serves as an internal reference. b. Dot blotting was used to detect the miR24-2. U6 serves as an internal reference. c. mature miR24-2 was detected by quantitative RT-PCR. U6 is used as an internal reference.**, $P < 0.01$, *, $P < 0.05$. I. The cell proliferation ability was determined by the CCK8. **, $P < 0.01$, *, $P < 0.05$. J. Plate colony formation ability was determined by crystal violet staining. K. The sphere formation ability of the cells.**, $P < 0.01$, *, $P < 0.05$. L. The hLCSCs were inoculated subcutaneously into Balb/C nude mice for 1 month. a. Photograph of

transplanted tumors (xenografts). b. Comparison of the size (g) of transplanted tumors in nude mice. c. Comparison of time (days) of transplanted tumors in nude mice (mean ± SEM, n = 6), **, $P < 0.01$, *, $P < 0.05$.

Figure S3 miR24-2 knockout identification. The DNA was isolated from hLCSCs stable infected with rLV-Cas9- miR24-2. The miR24-2 gRNA-intron fragment was analyzed by polymerase chain reaction, and β-actin was used as an internal reference gene. No band was shown if miR24-2 was knocked out. Positive miR24-2 knockout cell lines:2#,3#,6#,8#,11#,14#,15#,16#.

Figure S4 A. The Northern-Wstern blotting analysis of miR23a in rLV-Cas9 group and rLV-Cas9–miR24-2 group. **B.** The Northern-Western blotting analysis of miR27a in rLV-Cas9 group and rLV-Cas9–miR24-2 group

Figure S5 miR24-2 targets PRMT7 and inhibits HULC in human liver cancer stem cells. A. a. Northern-Western blotting was used to detect the miR24-2. U6 as an internal reference gene. b. Quantitative reverse transcription polymerase chain reaction (RT-PCR) was used to detect the miR24-2.U6 was used as an internal reference gene. B**.** The pEZX-MT-PRMT7 3'UTR(mutante)-Luc dual luciferase

reporter gene activity was tested. C.a. The miR24-2 was detected by Northern – Western blotting. U6 serves as an internal reference gene. b. Dot blotting was used to detect the miR24-2. GAPDH is used as an internal reference gene. c. The RT-PCR was performed to detect the mature miR24-2. U6 as an internal reference. D. The binding ability of the mature miR24-2, AgoII to PRMT7 3'-uncoding region (3'-UTR) was analyzed by RNA pulldown combined with RNA immunoprecipitation (RIP). E. The pEZX-MT-PRMT7 3'-UTR-Luc luciferase reporter gene activity was detected. F. The pEZX-MT-PRMT7 3'-UTR (mutant)-Luc luciferase reporter gene activity was detected . **, $P < 0.01$, *, $P < 0.05$. G. The PRMT7 was detected by RT-PCR and Western blotting. β-actin was used as an internal reference.

Figure S6 miR24-2 affects the modification of trimethylation of arginine-3 of histone H4 on the HULC promoter region specifically. A. the native CHIP primers were designed according to the HULC promoter sequence[AL133261.8 (1..66219)].

B .the modification of dimethylation of arginine-3 of histone H4 on the HULC promoter region was analyzed by native CHIP. C. B .the modification of

trimethylation of arginine-3 of histone H4 on the HULC promoter region was analyzed by native CHIP.

Figure S7 miR24-2 promotes expression and maturation of miR675 in stable human liver cancer stem cell lines (hLCSCs) infected with rLV-tet on-miR24-2 . A. rLV-tet on-miR24-2-infected stable human liver cancer stem cell lines (hLCSCs) were treated with different concentrations of DOX (0 μg/ml, 0.5 μg/ml, 1 μg/ml, 2 μg/ml), and then the total RNA was extracted. miR24-2 was detected by Northern blotting. U6 serves as an internal reference gene. b. mature miR24-2 was detected by quantitative reverse transcription polymerase chain reaction (RT-PCR). U6 is used as an internal reference gene. Each experiment was repeated three times. Each group of values is expressed as mean ± standard deviation (mean ± SEM, n = 3), **, $P < 0.01$, *, $P < 0.05$. B. Chromosome immunoprecipitation (CHIP) was performed using anti-Nanog, anti-HDAC4, anti-H3K9Ac, and anti-RNA polII. The polymer isolated and purified from the CHIP precipitate was used as a template, and polymerase chain reaction (PCR) amplification was carried out using a primer designed according to the Pri-miR675 promoter. IgG CHIP was used as a negative control; the DNA retained

before chromatin immunoprecipitation was used as a template, and the product amplified by the primer designed by the Pri-miR675 promoter was used as an internal reference (INPUT). C. Stable human hepatoma stem cell lines (hLCSCs) infected with rLV-tet on-miR24-2 (rLV-tet on-miR24-2 group) and rLV-tet on-miR24-2 infection + pGFP-V-RS-Nanog Transfected stable human hepatoma stem cell lines (hLCSCs) (rLV-tet on-miR24-2+pGFP-V-RS-Nanog group) were treated with different concentrations of DOX (1 μg/ml, 2 μg/ml). The binding ability of Nanog, HDAC4, H3K9Ac and RNA polII to the cis-miR675 promoter cis element was analyzed by chromatin immunoprecipitation (CHIP). D. a. The Super-DNA-protein complex gel Migration assay (Super-EMSA) using Biotin-labeled pri-miR675 promoter cis-element probe (Biotin-pri-miR675 promoter cis-element) and anti-RNA polII. Super-EMSA with IgG as a negative control, nucleoprotein-free EMSA and EMSA with excess cold probe as a system reference. b. Grayscale scan analysis of positive bands. E.a .The binding ability of RNApolII to the pri-miR675 promoter cis-element probe was analyzed using a Super-gel migration assay via biotin-labeled pri-miR675 promoter cis-element probe (Biotin-pri-miR675 promoter cis-element)

and anti-RNA polII, anti-Biotin. b. Grayscale scan analysis of positive bands. F. The stable human liver cancer stem cell lines (hLCSCs) infected with rLV-tet on-miR24-2 were treated with different concentrations of DOX (0 μg/ml, 0.5 μg/ml, 1 μg/ml, 1.5 μg/ml, 2 μg/ml).The pEZX-MT-Pri-miR675-Luc luciferase reporter gene plasmid carrying the pri-miR675 promoter was transfected into the above five stable liver cancer stem cell lines, and the activity of the luciferase reporter gene was detected 48 hours later. G. The stable human liver cancer stem cell lines (hLCSCs) infected with rLV-tet on-miR24-2 (rLV-tet on-miR24-2 group) and rLV-tet on-miR24-2 + pGFP-V-RS-Nanog were treated with different concentrations of DOX (0 μg/ml, 1 μg/ml, 2 μg/ml). The pEZX-MT-Pri miR675-Luc luciferase reporter plasmid carrying the pri-miR675 promoter was transfected into the above stable liver cancer stem cell lines, and the activity of the luciferase reporter gene was detected 48 hours later. Each experiment was repeated three times. Each group of values is expressed as mean ± standard deviation (mean ± SEM, n = 3), **, $P < 0.01$, *, $P < 0.05$.

Figure S8 miR675 targeted histone deacetylase HDAC3 in human liver cancer stem cell line. A. human liver cancer stem cell line (hLCSCs) was infected with

lentivirus rLV-miR675, lentivirus rLV, rLV-Cas9-miR675 and rLV-Cas9, respectively.Positive cells were screend and expanded. Then, total cellular RNA was extracted, and the miR675 in these four stable cell lines were detected by Northern blotting, U6 was used as an internal reference gene. **B.** Quantitative reverse transcription polymerase chain (RT-PCR) was used to detect the miR675 in these four stable cell lines, and U6 was used as an internal reference gene. **C.** Bioinformatics analysis of mature miR675 seed sequence binding to HDAC3 mRNA 3'-coding sequence (UTR) using MirTarget scanning soft software and BLAST tools. **D.** The pEZX-MT-HDAC3 3'-UTR-Luc luciferase reporter plasmid was transfected to the human liver cancer stem cell line hLCSCs and then the pEZX-MT-HDAC 3'-UTR-Luc dual luciferase reporter gene activity was detected. Each experiment was repeated three times. Each group of values is expressed as mean ± standard deviation (mean ± SEM, n = 3), **, $P < 0.01$, *, $P < 0.05$. **E**. Reverse transcription polymerase chain reaction (RT-PCR) was used to detect the transcriptional capacity of HDAC3 in these four stable cell lines, and β-actin was used as an internal reference gene. F.

Western blotting was used to detect the translational capacity of PRMT7 in these four stable cell lines, and β-actin was used as an internal reference gene.

FigureS9 miR24-2 enhances PI3K and affects autophagy in human liver cancer stem cells. A. chromosome immunoprecipitation(CHIP) with anti-H4K16Ac and anti-H3K20me2 were performed . B. The pGL4-PI3K-Luc luciferase reporter gene activity of the luciferase reporter gene was detected .**, $P < 0.01$, *, $P < 0.05$. C. The RT-PCR analysis was performed . β- actin serves as an internal reference gene. D. Western blotting with anti-PI3K was performed. β-actin as an internal reference gene. E. The RT-PCR was ued to detect PI3K . β-actin was used as an internal reference gene. F. Western blotting was performed using anti-PI3K. β-actin was used as an internal reference gene. **G**. The co-immunoprecipitation with anti-LC3 and the precipitate was analyzed by Western blotting with anti-ATG4.H. Western blotting was performed using anti-LC3.β-actin was used as an internal reference gene. I. The co-immunoprecipitation with anti-ATG3. J. Western blotting with anti-Beclin1. K. The infection of adenovirus rAd-Cherry-GFP-LC3 can monitor the autophagy through fluorescence microscopy directly. The occurrence of autophagy was observed (red

marker Cherry-LC3). L. a. Infection of adenovirus rAd-Cherry-GFP-LC3 can monitor the autophagy directly by fluorescence microscopy (red marker Cherry-LC3). b. Comparison of the incidence of autophagy. **, $P < 0.01$, *, $P < 0.05$.

Figure S10 miR24-2 affects expression. of PI3K dependent HDAC3-H4K16Ac-H4K20me2 in human liver cancer stem cells. A.a. The binding ability of H3K20me2 to the PI3K promoter cis-element probe was determined by Super-DNA-protein complex gel migration assay (Super-EMSA) using Biotin-labeled PI3K promoter cis-element probe (Biotin-PI3K promoter cis-element) and anti-H4K20me2, anti-Biotin. IgG super-EMSA was used as a negative control, EMSA without nucleoprotein and EMSA with excess cold probe were used as system reference, and the hybridization band of cis element of Biotin-PI3K promoter and the amount of nucleoprotein added were used as INPUT. b. Grayscale scan analysis of positive bands. B. a. The stable human liver cancer stem cell lines (hLCSCs) infected with rLV-tet on -miR24-2 and rLV-tet on-miR24-2+pcDNA3-HDAC3 were treated with different concentrations of DOX (0 μg/ml, 1 μg/ml, 2 μg/ml). The nuclear protein was extracted and the binding ability of RNApolII to the PI3K promoter

cis-element probe was determined by Super-gel migration. Super-DNA-protein complex gel migration assay (Super-EMSA) using Biotin-labeled PI3K promoter cis-element probe (Biotin-PI3K promoter cis-element) and anti-RNApolII, anti-Biotin IgG super-EMSA was used as a negative control, EMSA without nucleoprotein and EMSA with excess cold probe were used as system reference, and the hybridization band of cis element of Biotin-PI3K promoter and the amount of nucleoprotein added were used as INPUT. b. Grayscale scan analysis of positive bands. C. The pGL4-PI3K-Luc luciferase reporter gene plasmid was transfected into these stable liver cancer stem cell lines, and the activity of the luciferase reporter gene was detected 48 hours later. Each experiment was repeated three times. Each group of values is expressed as mean ± standard deviation (mean ± SEM, n = 3), **, $P < 0.01$, *, $P < 0.05$. D. The reverse transcription polymerase chain reaction (RT-PCR) using PI3K primers, and β-actin was used as an internal reference gene. E. The stable human liver cancer stem cell lines (hLCSCs) infected with rLV-tet on-miR24-2 + pGFP-V-RS-KAT8 , rLV-tet on-miR24-2 + pcDNA3-SET8 were treated with different concentrations of DOX (0μg/ml, 2μg/ml), and reverse transcription

polymerase chain reaction (RT-PCR) was performed using PI3K primers. β-actin as an internal reference gene. F. Western blotting with anti-PI3K, anti-KAT8, anti-SET8, anti-H4K16Ac and anti-H4K20me2, β-actin as internal Reference gene. G. Western blotting with anti-PI3K, anti-KAT8, anti-SET8, anti-H4K16Ac and anti-H4K20me2. β-actin is used as an internal reference gene.

Figure S11 miR24-2 increases autophagy dependent on phosphatidylinositol 3-kinase (PI3K) to in human liver cancer stem cells. A. The human livrer cancer stem cell lines (hLCSCs) transfected with pCMV-miR,pCMV-miR24-2 and pCMV-miR24-2+pGFP-V-RS-PI3K ,respectively, the total protein in the cell line was stabilized, and Western blotting was performed using anti-LC3 and anti-PI3K, and β-actin was used as an internal reference gene. B. Stable human liver cancer stem cell lines (hLCSCs) infected with rLV-tet on-miR24-2 and rLV-tet on-miR24-2 + pGFP-V-RS-PI3K, respectively, were treated with different concentrations of DOX (0 μg/ml, 2 μg/ml), and then total cellular proteins were extracted, and Western blotting was performed using anti-LC3 and anti-PI3K, and β-actin was used as an internal reference gene. C.The human liver cancer stem cell line infected with rLV-tet

on-miR24-2 and rLV-tet on -miR24-2 infection + pGFP-V-RS-KAT8 or pcDNA3-SET8 were treated with different concentrations of DOX (0 μg/ml, 2 μg/ml), and then total cellular proteins were extracted, western blotting was performed using anti-LC3, and β-actin was used as an internal reference gene. D. The experimental samples were co-immunoprecipitated with anti-ATG3, and the precipitates were analyzed by Western blotting with anti-LC3. IgG co-immunoprecipitation was used as a negative control, and the sample before coprecipitation was subjected to Western blotting with anti-ATG3 as INPUT. E. Stable human liver cancer stem cell lines (hLCSCs) infected with rLV-tet on-miR24-2 and rLV-tet on-miR24-2 infection + pGFP-V-RS-PI3K, respectively were treated with different concentrations of DOX (0 μg/ml, 2 μg/ml), then the total protein of the cells was extracted.The experimental samples were co-immunoprecipitated with anti-ATG3, and the precipitate was immunoblotted with anti-LC3. IgG co-immunoprecipitation was used as a negative control, and the sample before coprecipitation was subjected to Western blotting with anti-ATG3 as INPUT. F. human liver cancer stem cell lines (hLCSCs) transfected pCMV-miR pCMV-miR24-2 and pCMV-miR24-2+pGFP-V-RS-PI3K,respectively.

Western blotting was performed using anti-Beclin1, and β-actin was used as an internal reference gene. G. Stable human liver cancer stem cell lines (hLCSCs) infected with rLV-tet on-miR24-2 and rLV-tet on-miR24-2 infection+ pGFP-V-RS-PI3K were treated with different concentrations of DOX (0 μg/ml, 2 μg/ml) and then total cellular proteins were extracted.Western blotting was performed using anti-Beclin1, and β-actin was used as an internal reference gene. H. a. Human liver cancer stem cell lines (hLCSCs) transfected with pCMV-miR , pCMV-miR24-2, and pCMV-miR24-2+pGFP-V-RS-PI3K ,respectively. The infection of the adenovirus rAd-Cherry-GFP-LC3 was able to monitor the autophagy directly by fluorescence microscopy (red marker Cherry-LC3). b. Comparison of the incidence of autophagy in cells. Each experiment was repeated three times. Each group of values is expressed as mean ± standard deviation (mean ± SEM, n = 3), **, $P < 0.01$, *, $P < 0.05$. I.a .human liver cancer stem cell lines (hLCSCs) infected with rLV-tet on-miR24-2 and rLV-tet on-miR24-2 + pGFP-V-RS-PI3K,respectively were treated with the concentration of DOX (0μg/ml, 2μg/ml).The adenovirus rAd-Cherry-GFP-LC3, which can monitor autophagy, was directly infected, and then

the autophagy occurred after cell starvation was directly observed by fluorescence microscope (red marker Cherry-LC3). b. Comparison of the incidence of autophagy in cells. Each experiment was repeated three times. Each group of values is expressed as mean ± standard deviation (mean ± SEM, n = 3), **, $P < 0.01$, *, $P < 0.05$.

Figure S12 4% formaldehyde-fixed, paraffin-embedded transplanted tumor tissue section (4 μm) was subjected to hematoxylin-eosin (HE) (original magnification × 100).

Figure S13 The molecular mechanism that miR24-2 promotes malignant growth of liver cancer stem cells. miR24-2 enhances the expression and function of the tyrosine protein kinase sarcoma gene Src in liver cancer stem cells and promotes the malignant growth of liver cancer stem cells. First, the mature sequence of miR24-2 binds to the protein arginine methyltransferase 7 (PRMT7) mRNA 3' noncoding region (UTR) and thus inhibits the translational ability of the *PRMT7* gene. Then, miR24-2 inhibited the bi- (tri)methylation of histone 4 arginine by reducing

PRMT7 (H4R3me2 and H4R3me3), significantly reducing the binding capacity of H4R3me2 and H4R3me3 to HULC promoter, promoting HULC expression. miR24-2-dependent HULC promoted the binding of C-myc, Epcam and KLF4 to the Nanog promoter in human hepatoma stem cells, and promoted its transcriptional activity and expression. Moreover, miR24-2 inhibits the expression of histone deacetylase HDAC3 in human hepatoma stem cells through miR675, and promotes the acetylation of lysine at position 16 of Histone H4 in human liver stem cells, and relies on the 16th lysine of Histone H4. The acetylation modification of the acid inhibits the methylation modification of the 20th lysine of Histone H4. Moreover, miR24-2 increased histone H4K16Ac and attenuated the binding ability of H4K20me2 to enhance expression of PI3K. Subsequently, miR24-2 is dependent on PI3K to enhance the expression of autophagy structural protein LC3 and its interaction with the cleavage protein ATG4. Thereby, LC3 is further matured into activated LC3II, and the interaction between LC3II and processing protein ATG3. Then miR24-2 enhances the interaction between PKM1 and autophagosome functional protein P62, and enhances the protection of PKM1 by autophagy of liver

cancer stem cells, and inhibits the degradation of PKM1.Interestingly, miR24-2 promotes the binding of PKM1 to the tyrosine protein kinase sarcoma gene Src promoter and enhances the the expression of *Src*. Moreover, the *Src* gene plays an important role in the malignant growth of human liver cancer stem cells triggered by miR24-2.

Supplemental Figure

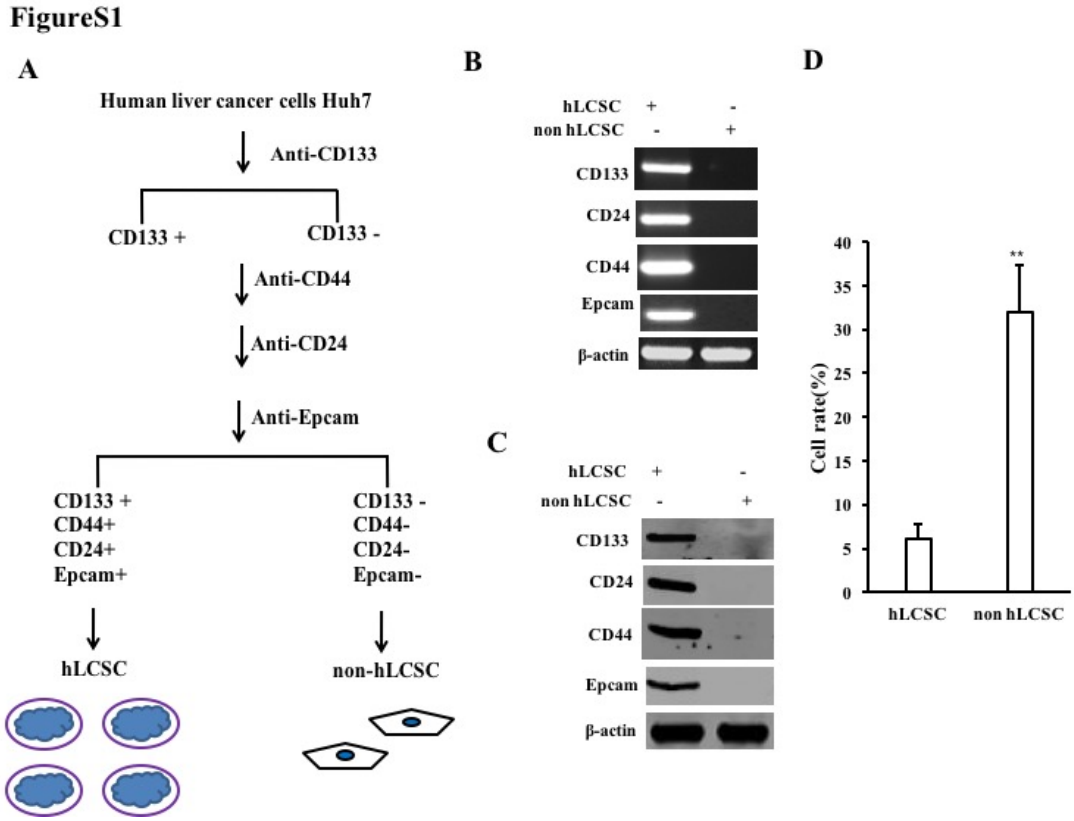

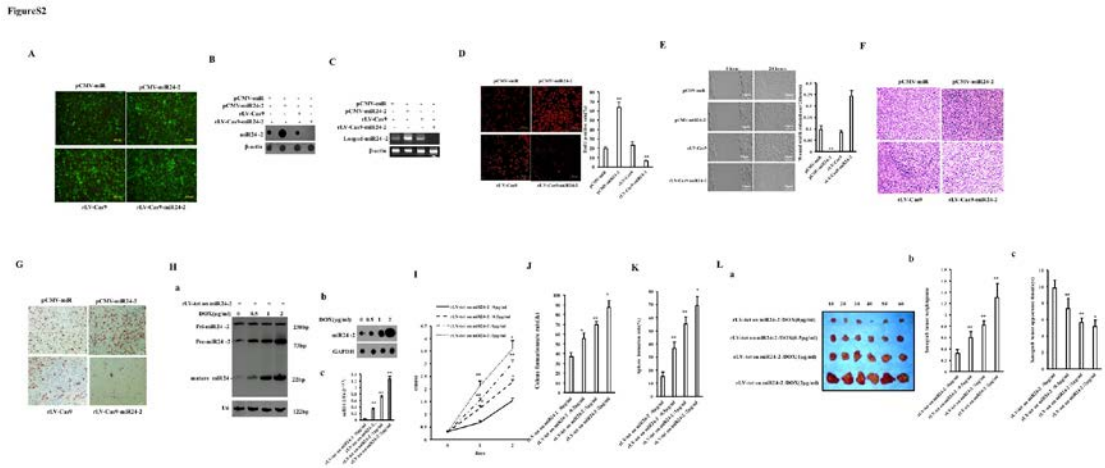

FigureS3

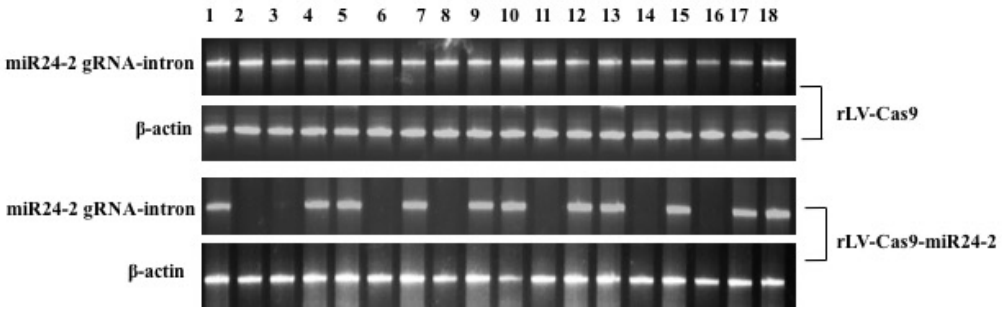

FigureS4

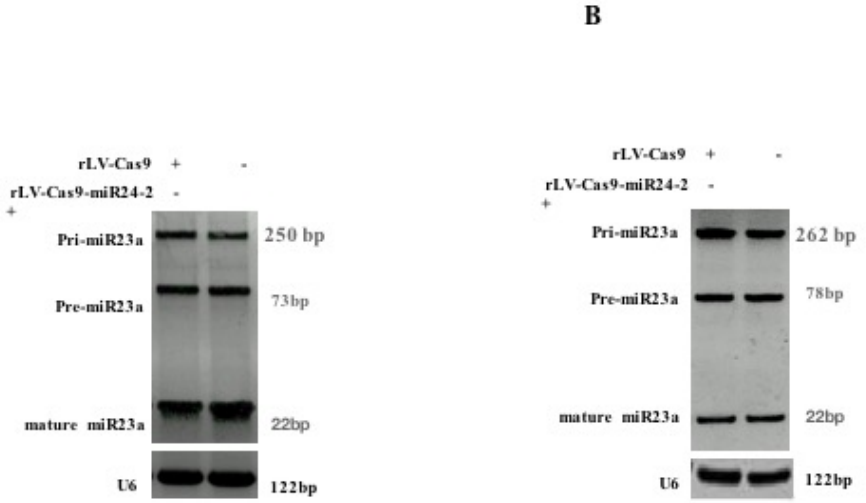

Figure S5

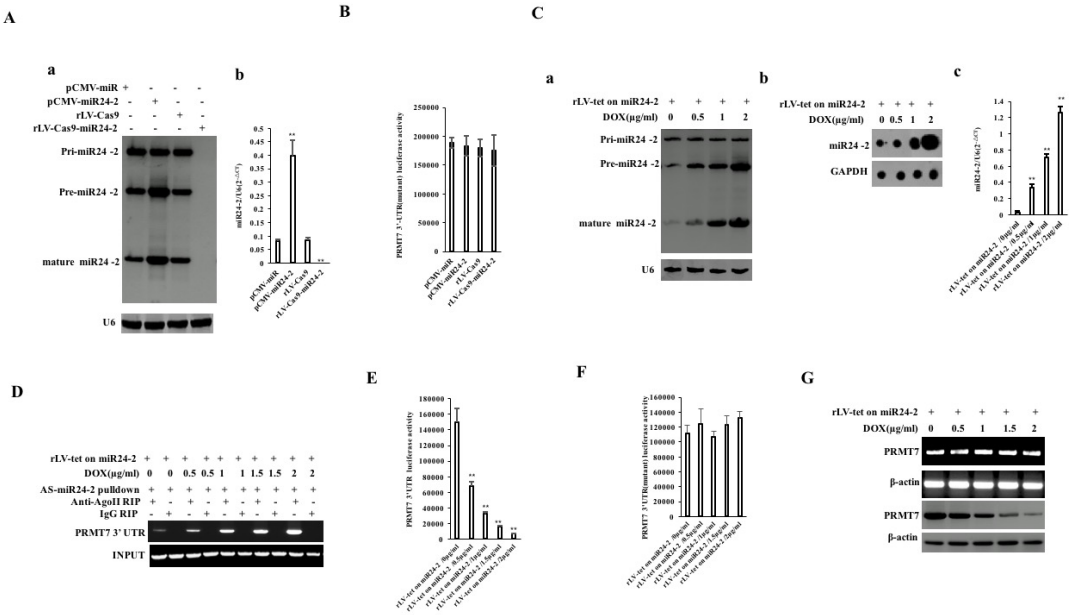

FigureS6

A

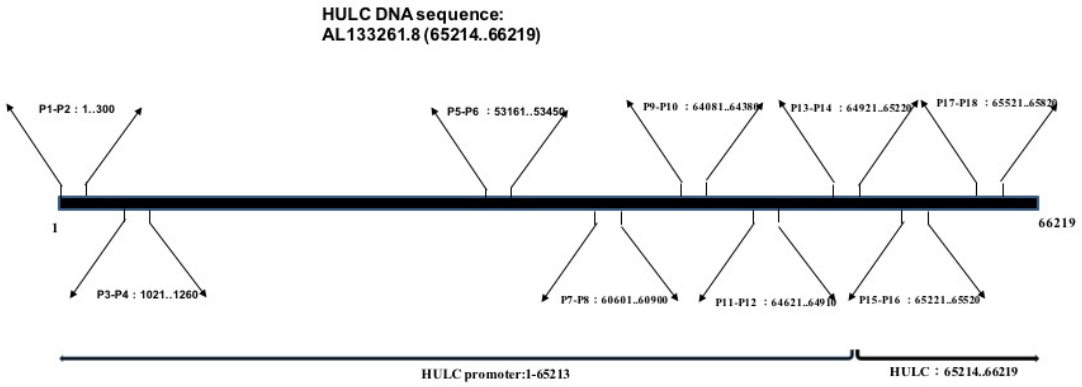

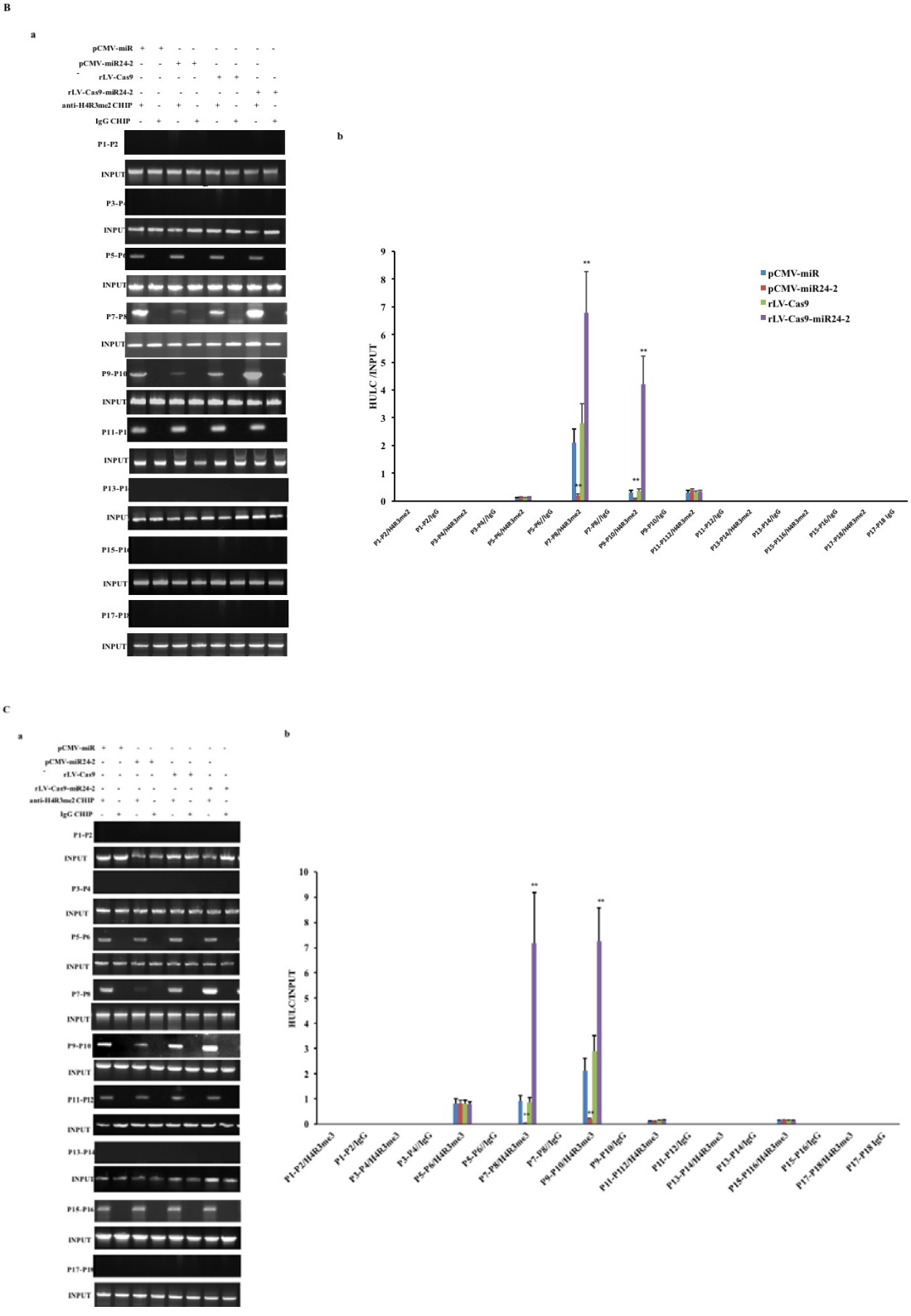
B
a
pCMV-miR
pCMV-miR24-2
rLV-Cas9
rLV-Cas9-miR24-2
anti-H4R3me2 CHIP
IgG CHIP
P1-P2
INPUT
P3-P4
INPUT
P5-P6
INPUT
P7-P8
INPUT
P9-P10
INPUT
P11-P12
INPUT
P13-P14
INPUT
P15-P16
INPUT
P17-P18
INPUT
b
HULC /INPUT
pCMV-miR
pCMV-miR24-2
rLV-Cas9
rLV-Cas9-miR24-2
P1-P2/H4R3me2
P1-P2/IgG
P3-P4/H4R3me2
P3-P4/IgG
P5-P6/H4R3me2
P5-P6//IgG
P7-P8/H4R3me2
P7-P8//IgG
P9-P10/H4R3me2
P9-P10/IgG
P11-P12/H4R3me2
P11-P12/IgG
P13-P14/H4R3me2
P13-P14/IgG
P15-P116/H4R3me2
P15-P16/IgG
P17-P18/H4R3me2
P17-P18 IgG
C
a
pCMV-miR
pCMV-miR24-2
rLV-Cas9
rLV-Cas9-miR24-2
anti-H4R3me2 CHIP
IgG CHIP
P1-P2
INPUT
P3-P4
INPUT
P5-P6
INPUT
P7-P8
INPUT
P9-P10
INPUT
P11-P12
INPUT
P13-P14
INPUT
P15-P16
INPUT
P17-P18
INPUT
b
HULC/INPUT
P1-P2/H4R3me3
P1-P2/IgG
P3-P4/H4R3me3
P3-P4/IgG
P5-P6/H4R3me3
P5-P6//IgG
P7-P8/H4R3me3
P7-P8//IgG
P9-P10/H4R3me3
P9-P10/IgG
P11-P12/H4R3me3
P11-P12/IgG
P13-P14/H4R3me3
P13-P14/IgG
P15-P116/H4R3me3
P15-P16/IgG
P17-P18/H4R3me3
P17-P18 IgG

FigureS7

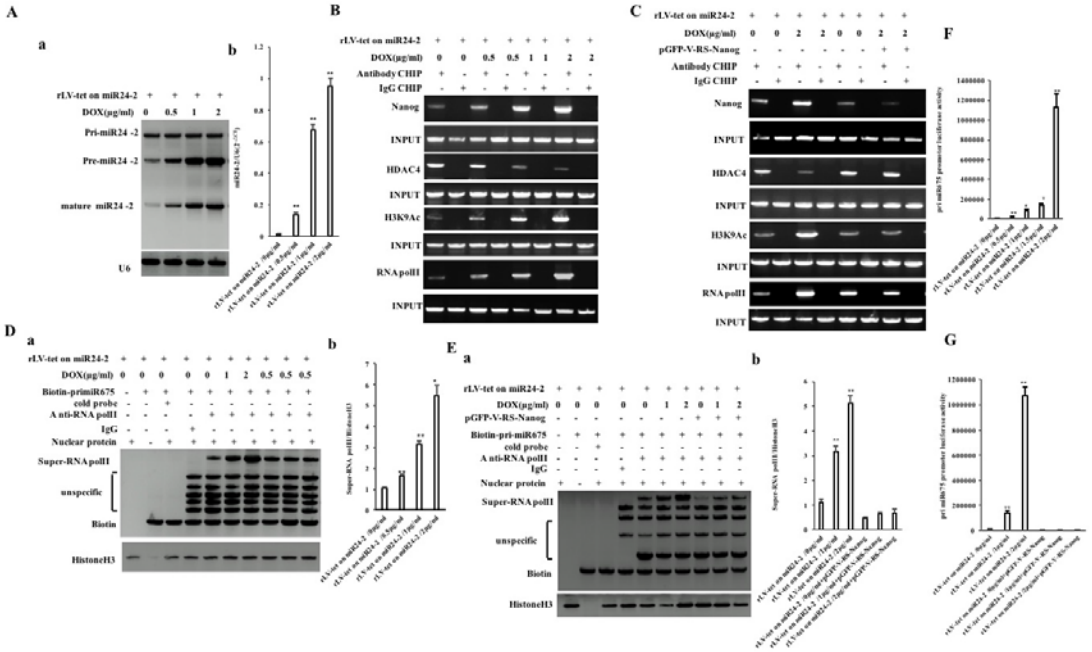

FigureS8

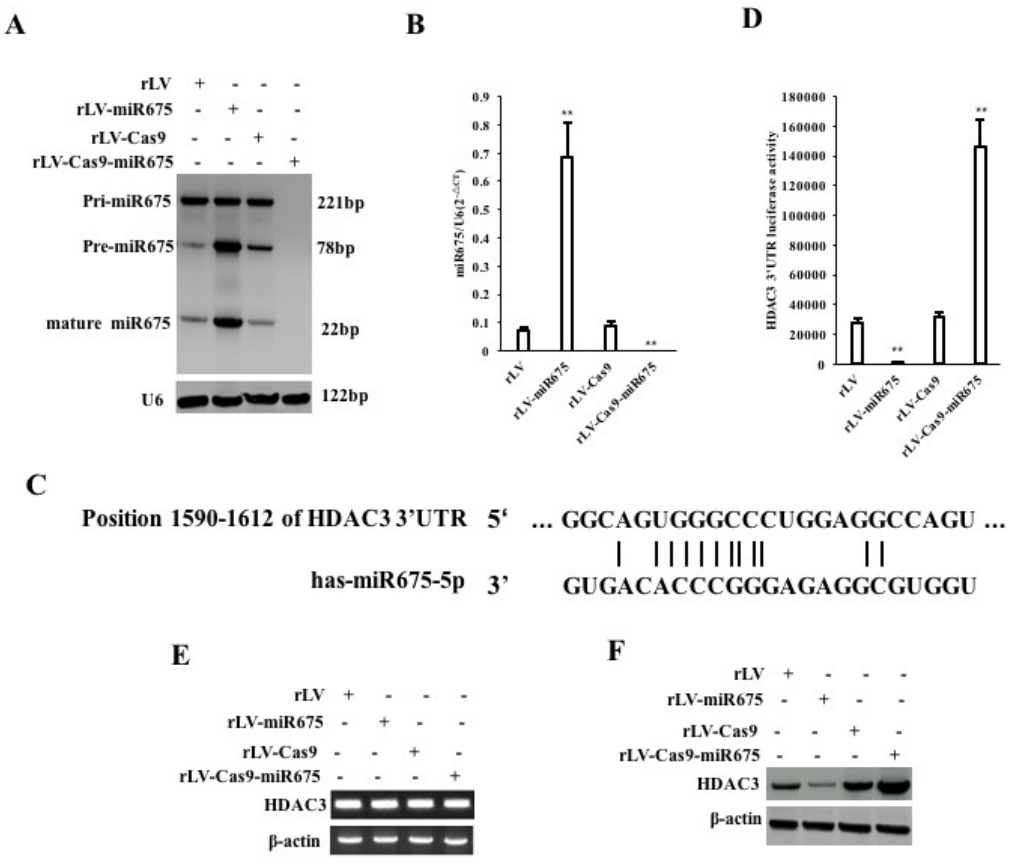

FigureS9

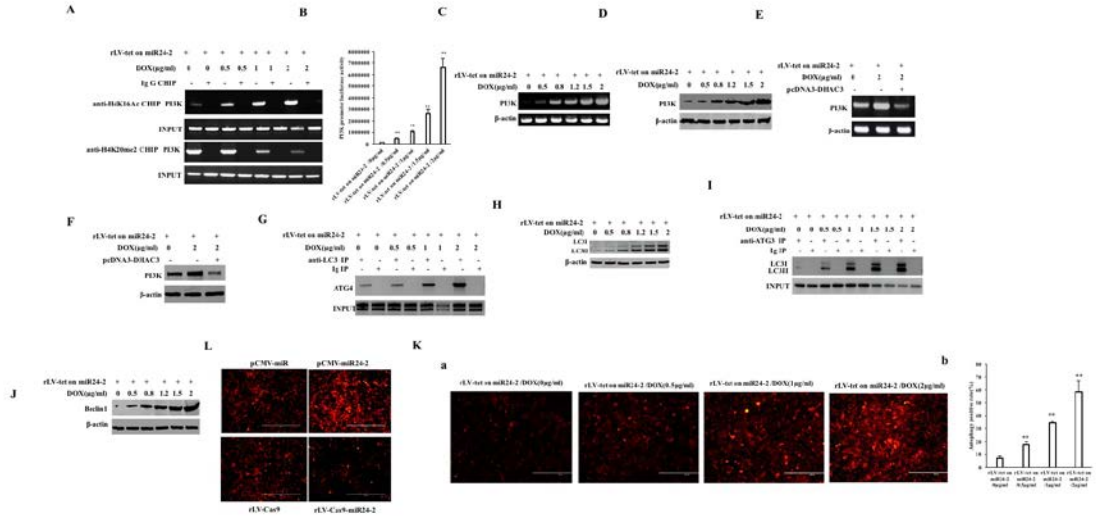

FigureS10

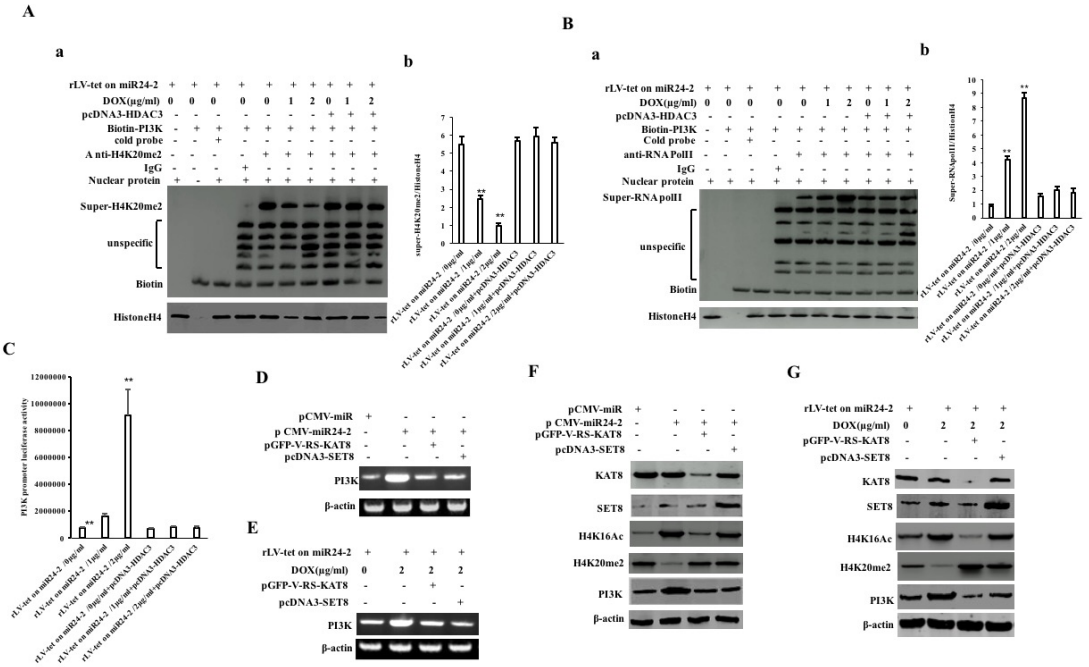

FigureS11

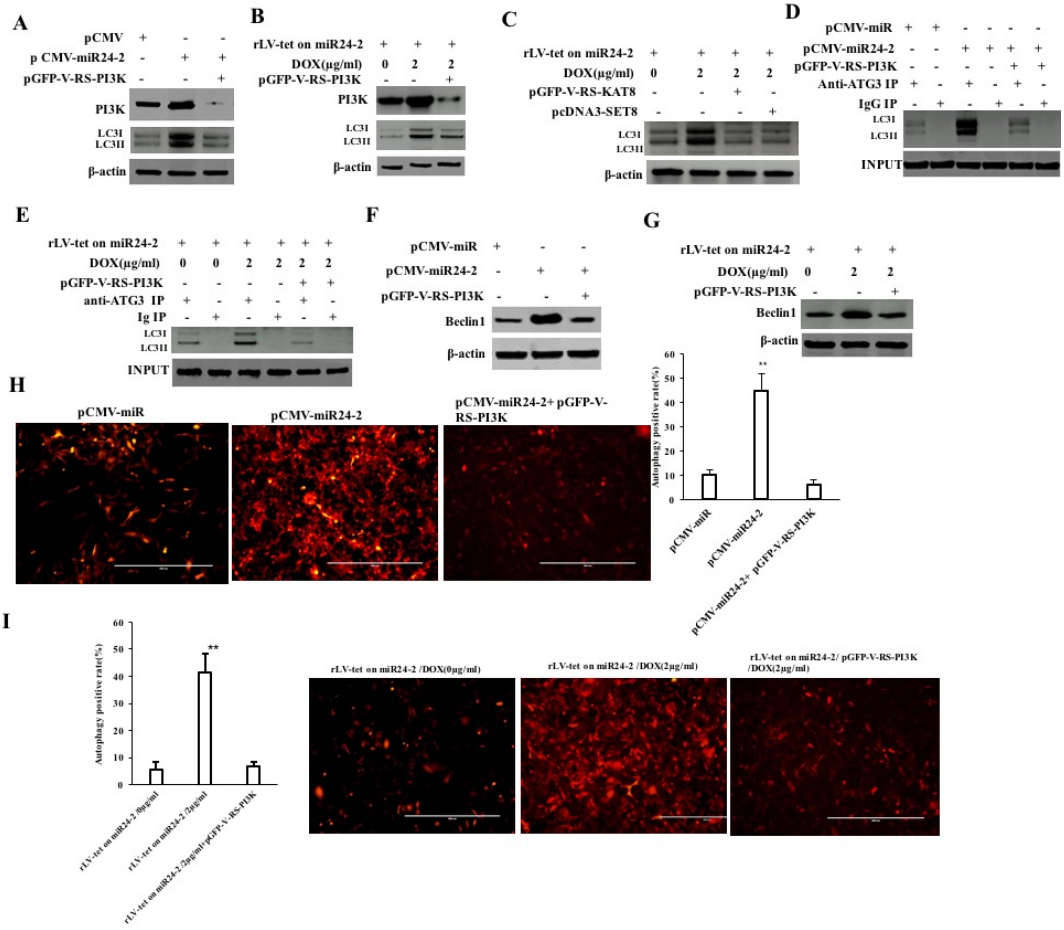

FigureS12

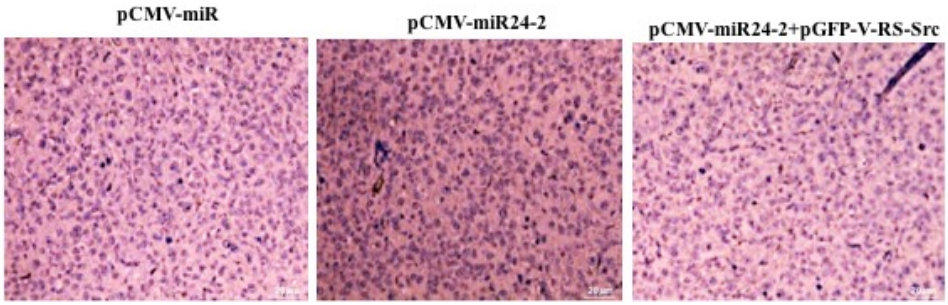

FigureS13

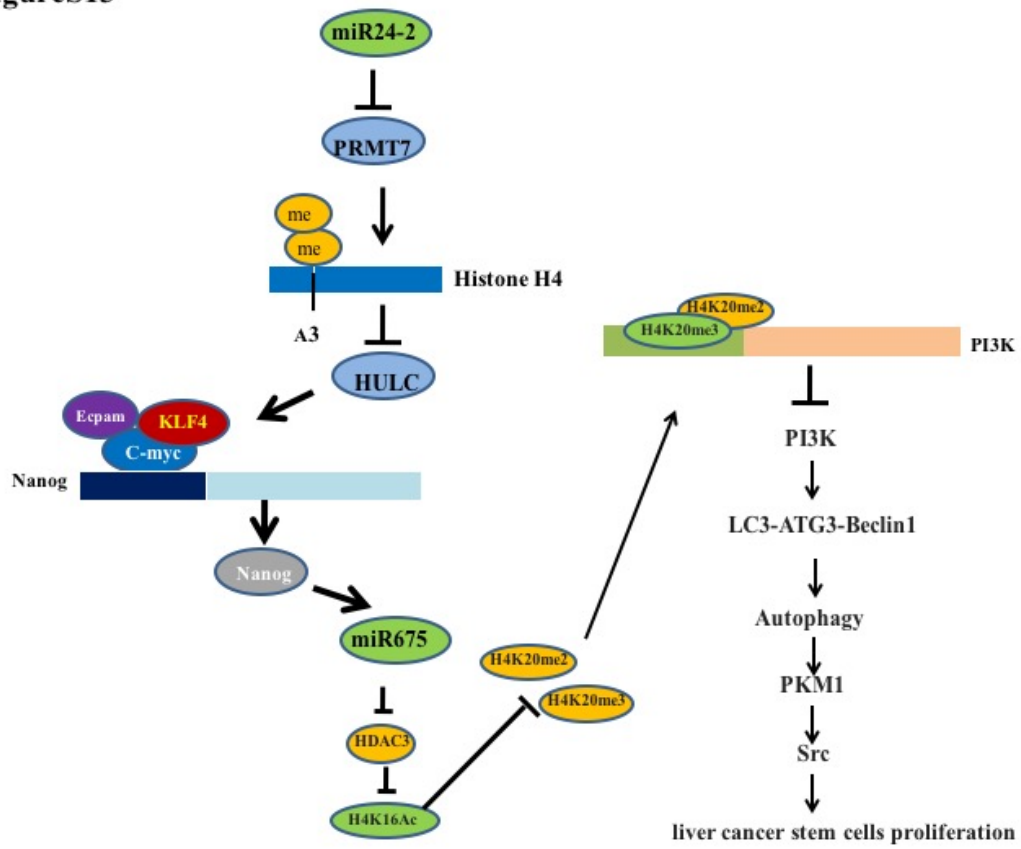
miR24-2
PRMT7
me
me
Histone H4
A3
HULC
Ecpam
KLF4
C-myc
Nanog
Nanog
miR675
HDAC3
H4K16Ac
H4K20me2
H4K20me3
H4K20me2
H4K20me3
PI3K
PI3K
LC3-ATG3-Beclin1
Autophagy
PKM1
Src
liver cancer stem cells proliferation